

**SECOND ORDER ASYMPTOTICS FOR PROPELLER  
NOISE AND APPLICATION TO HELICOPTER  
ROTOR BLADES**

**M.Sc. Thesis by  
Baha ZAFER, B.Sc.**

**708021011**

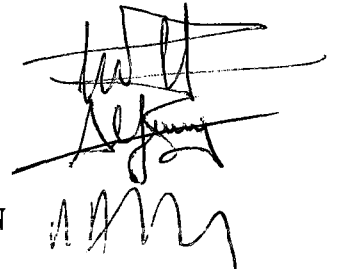
**Date of submission : 9 May 2005**

**Date of defence examination: 30 May 2005**

**Supervisor (Chairman): Prof. Dr. Can F. DELALE**

**Members of the Examining Committee Prof.Dr. Adil YÜKSELEN**

**Prof.Dr. A. Rüstem ASLAN**

Handwritten signatures of the supervisors and committee members. The first signature is for Prof. Dr. Can F. DELALE, the second for Prof. Dr. Adil YÜKSELEN, and the third for Prof. Dr. A. Rüstem ASLAN.

**MAY 2005**

## **PREFACE**

Many people have made contributed to this work. My supervisor Prof. Dr. Can F. Delale has followed my research from its early to its final stages by giving me advise and providing guidance. I am certain that these years, nearly two, working under his guidance will have an influence on my scientific vision, especially when thinking about mathematics.

I would like to thank Prof. Dr. R. Alsan Meriç for his support in the beginning of my graduate education by advising me in the choice of graduate courses and helping me in preparing of my first proceeding paper.

Special thanks are to Prof. Dr. A. Rüstem Aslan who provided me with data of aerodynamic loading in my aeroacoustic computation. I would like to thank Yrd. Doç. Dr. N.L. Okşan Çetiner-Yıldırım for her encouragement to enter this program.

Finally, my deepest gratitude goes to my family, who never ceased to give me support, especially my mother and father, to whom I dedicate this thesis.

This work was supported in part by Turkish Prime Ministry State Planning Organization (DPT) under program of Advanced Technologies Research and Education Program, project number: 2001K120750 90-146.

MAY 2005

Baha ZAFER

## **TABLE OF CONTENTS**

<b>LIST OF FIGURES .....</b>	<b>iv</b>
<b>SYMBOL LIST .....</b>	<b>v</b>
<b>ÖZET.....</b>	<b>vi</b>
<b>SUMMARY .....</b>	<b>vii</b>
<b>1. INTRODUCTION.....</b>	<b>8</b>
<b>2. EARLY THEORETICAL DEVELOPMENTS .....</b>	<b>11</b>
<b>3. THEORETICAL BACKGROUND.....</b>	<b>14</b>
3.1 Lighthill's acoustic analogy .....	14
3.2. The Ffowcs Williams–Hawkings equation .....	16
<b>4. AERODYNAMIC COMPUTATION .....</b>	<b>19</b>
<b>5. ASYMPTOTIC THEORY OF PROPELLER NOISE.....</b>	<b>22</b>
5.1. Hanson integral formula.....	22
5.2. First order asymptotic approximation .....	24
5.3. Second order asymptotic approximation.....	27
<b>6. RESULTS AND DISCUSSION .....</b>	<b>30</b>
<b>7. CONCLUSION.....</b>	<b>36</b>
<b>REFERENCES.....</b>	<b>38</b>

## LIST OF FIGURES

Figure 1.1: Helicopter Noise Classification.....	8
Figure 4.1: Detailed airfoil description.....	19
Figure 4.2: Boundary condition for aerodynamic calculation .....	20
Figure 5.1: Propeller geometry in the disk plane.....	23
Figure 6.1: $C_p$ distribution of 3-to-1 tapered tip blade along chordwise direction at $r/R_0=0.225$ .....	30
Figure 6.2: $C_p$ distribution of 3-to-1 tapered tip blade along chordwise direction at $r/R_0=0.775$ .....	31
Figure 6.3: $C_p$ distribution of 3-to-1 tapered tip blade along chordwise direction at $r/R_0=0.945$ .....	32
Figure 6.4: $C_p$ distribution of rectangular planform blade along radial direction in hover for the computation of noise prediction .....	32
Figure 6.5: Source strength $S_m(z)$ distribution for aerodynamic loading along spanwise direction.....	33
Figure 6.6: Polynomial fitting of the source strength $S_m(z)$ for aerodynamic loading by the method of least squares (NU is the degree of the polynomial) .....	33
Figure 6.7: Comparison of asymptotic predictions for aerodynamic loading between Parry-Crighton [3] and the present work for the SPL (dB) for an observer located at $r_o=141.421$ m with a radiation angle $\theta=89.88^\circ$ .....	34
Figure 6.8: Comparison of harmonic convergence at tip Mach number $M_t=0.5$ between Parry-Crighton [3] and the present work for the SPL (dB) for an observer located at $r_o=141.421$ m with a radiation angle $\theta=89.88^\circ$ for higher harmonic numbers.....	35

## SYMBOL LIST

$b$	: maximum airfoil thickness
$B$	: number of blades
$c$	: airfoil chord
$c_0$	: ambient speed of sound
$C_L$	: lift coefficient
$D$	: propeller diameter
$F_L$	: normalized lift distribution
$h$	: normalized thickness distribution
$k_y, k_x$	: wave numbers given by Eq. (5.4) and (5.5)
$m$	: harmonic number
$M_r$	: section relative Mach number
$M_t$	: tip rotational Mach number
$M_x$	: flight Mach number
$p$	: acoustic pressure
$p_m$	: normalized harmonic pressure coefficient
$r_0$	: distance from origin to observer
$S$	: source strength
$t$	: observer time
$X$	: normalized chordwise coordinate
$z$	: normalized radial coordinate
$\beta$	: a conveniently defined parameter given by Eq. (5.2.6)
$\theta$	: radiation angle from propeller axis to observer point
$v$	: power of the coordinate near the blade tip and define in Eq (5.2.7)
$\rho$	: acoustic density field
$\rho_0$	: ambient density
$\Phi_s$	: phase lag due to sweep, Eq. (5.6)
$\Psi_0$	: circumferential angle
$\Psi_L, \Psi_v$	: chordwise noncompactness factors
$\Omega$	: shaft angular speed
$\delta(-)$	: Dirac Delta Function
$v_n$	: local normal velocity of surface
$H(-)$	: Heaviside Function
$l_i$	: the local force vector exerted by the surface on the fluid
$T_{ij}$	: Lighthill's stress tensor
$R$	: blade radius
$\alpha$	: see Eq. (5.3.14)
$\lambda$	: $mB$ (the product of harmonic number $m$ by the blade number $B$ )
$C_t$	: thrust coefficient
$W_{out}$	: normalized outflow velocity of computational domain
$W_{in}$	: normalized inflow velocity of computational domain

## PERVANE GÜRÜLTÜSÜ İÇİN İKİNCİ MERTEBEDEN YAKLAŞIKLIK VE HELİKOPTER PALALARINA UYGULANMASI

### ÖZET

Bu çalışma uzak alanda  $B$ -palalı sesaltı dönel pervane için akustik basınçın  $m$ . harmonik bileşenini hesaplamaktadır ( $mB \rightarrow \infty$  yaklaşıklık limitinde). Parry ve Crighton sesaltı pervane gürültüsü için, profil kalınlığı ve aerodinamik yüklere ait ses kaynaklarını içeren yaklaşıklık bağıntıları ortaya koydular. Bu bağıntılar zamandan bağımsız aerodinamik yükler ile palaya ait kalınlık dağılımının sadece pala üzerindeki etkilerini içeren yüksek mertebeden Bessel fonksiyonları için Debye yaklaşımı ile bulunan integral denklemlere uygulanan Laplace yöntemi ile elde edilmiştir. Bunlara bağlı olarak, hesaplamalı akışkanlar mekaniğinde kullanılan metodlarla, temel alan yazılımları kullanılarak elde edilen aerodinamik yükler, bir polinomla betimlenerek Parry ve Crighton'a ait  $m$ . basınç harmoniği bağıntısı ikinci mertebeden bir düzeltme ile sesaltı pervane gürültüsünün  $m$ . harmoniği için genelleştirilmiştir.

Bu bağıntıların helikopter palasının uzak alan gürültüsü tayininde uygulanabilmesi için örnek olarak, askı durumunda iken pala uç Mach sayıları 0.5 ile 0.7 değerleri arasında değişen dört palalı bir helikopter pervanesi seçilmiştir. Bu durumda, üç boyutlu sonlu hacimler yöntemini temel alan hesaplamalı akışkanlar mekaniği yazılımı kullanılarak aerodinamik yükler hesaplanmış ve bu hesaplardan çıkan sonuçlarla kaynak şiddetleri polinom olarak seçilmiş bir bağıntıya göre belirlenmiştir. Parry ve Crighton'a ait bağıntı ile bu çalışmada ortaya konan ikinci mertebe yaklaşıklık bağıntısı kullanılarak yapılan hesaplar karşılaştırıldığında, sonuçların uyumlu olduğu görülmüştür. Özellikle, SPL değerlerine ait sonuçlarda, daha önceki çalışmalarda gözlemlenen sayısal sonuçlara yaklaşmayı daha iyi ifade eden bir azalma gözlenmiştir.

## SECOND ORDER ASYMPTOTICS FOR PROPELLER NOISE AND APPLICATION TO HELICOPTER ROTOR BLADES

### SUMMARY

This study provides asymptotic formulas for the far field of the  $m$ th harmonic components of the acoustic radiation from a  $B$ -bladed subsonic single rotational propeller, in the asymptotic limit as  $mB \rightarrow \infty$ . Asymptotic expressions of subsonic propeller noise of Parry and Crighton [3] accounting for contributions from airfoil thickness and loading are refined. These expressions are found by the application of Laplace's method to the integrals of steady loading and of blade thickness distributions over the surface of the blade using the Debye approximation. In particular, second order correction to single rotational propeller noise expression of Parry and Crighton is obtained for the harmonic components  $P_m$  of the subsonic propeller noise.

As an application, a four bladed helicopter rotor in hover with tip Mach numbers ranging between 0.5 and 0.7 is considered. A 3D compressible CFD code based on finite volume method is used to determine the aerodynamic loading and the results are fitted to define the source strength. Favorable agreements are found between the Parry and Crighton expression and the present formula with polynomial source distribution. It is demonstrated that the SPL noise prediction are reduced according to the present formula, showing a shift towards agreement with full numerical computations, previously demonstrated by Parry and Crighton.

## 1. INTRODUCTION

Noise has been an undesirable phenomenon of aerospace vehicles from the time of early aircraft until now. Especially, rotorcrafts are inherently more complex aeromechanical vehicles than aircrafts. For instance, the operating environment of a helicopter rotor is extremely complex and fundamentally unsteady. This complicated aeromechanical environment contributes to both discrete frequency and to broadband aerodynamic noise generation through several distinct noise mechanisms. Discrete-frequency noise is usually divided into the deterministic components of thickness and loading noise, blade-vortex interaction noise and high-speed impulsive noise. Similarly, broadband noise consists of the non-deterministic loading noise sources classified as turbulence ingestion noise, blade-wake interaction noise and blade self-noise [1]. Other exterior noise sources, such as engine noise, and interior noise sources, such as drive-train and gear noise, are also important rotorcraft noise sources, but they are not considered here. The various types of helicopter noise are given below in Figure 1.1.

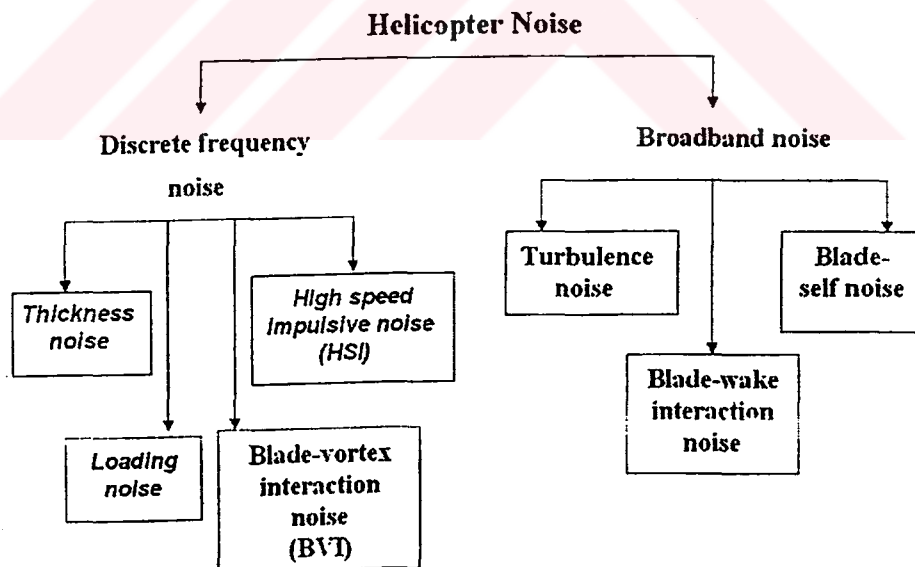


Figure 1.1: Helicopter Noise Classification



Thickness noise and loading noise, known together as rotational noise, are related to linear aerodynamic theory. In this theory quadrupole effects are neglected completely. Thickness noise is due to the displacement of the fluid in the flow field by the rotor blade, and loading noise is caused by the accelerating force on the fluid generated by the moving blade surface. Blade-vortex interaction noise (BVI) occurs as a result of the tip vortex interacting with the blade. At high advancing tip speeds, the rotor generates impulsive noise of high intensity, called high speed impulsive noise (HSI).

Essentially all broadband noise is generated by random loading on the rotor blade. Broadband noise can be generated by turbulence phenomena associated with the flow near or on the blade surface that is usually called turbulence noise. In the helicopter rotor noise frequency spectrum, the mid to high frequency range is generally of broadband nature. The mid-frequency broadband noise is produced by blade-wake interaction (BWI). BWI noise is produced when the rotor blade encounters the wake turbulence, usually of preceding blades. This situation appears in level flight and mild climb conditions. The high-frequency broadband noise is mostly self-noise, i.e., the noise produced by boundary layer turbulence and the shedding of turbulent eddies at the trailing edge.

The ability to predict noise generated from rotational sources, e.g. propeller or helicopter rotor, is important. Several approaches to the problem have been used in the past, including numerical and experimental studies. The errors which are always present in numerical solutions can generate more noise than the 'real' flow field. Consequently, analytical methods not only work well, but they are often preferred to computational ones. The acoustic analogy is widely used as an analytical model to investigate fundamental aeroacoustic aspects approximately. Fluid dynamic processes which generate sound are usually confined to a more or less clearly defined region which is identified as a source for noise generation. Serious difficulties are encountered in computing the noise generated by this source.

The main division in noise prediction theories is frequency domain and time domain methods. A frequency domain method is one which predicts the strength of each harmonic of the noise from a source directly. On the other side, a time domain method

yields a time record, typically for one revolution of the source. As a result, there is no particular preferred method for low speed and low blade number rotors. For rotors with many blades, frequency domain methods are more efficient. Conversely, for very high speed rotors, time domain techniques are faster [2]. In general, frequency domain methods are more elegant and easier, especially for mathematical analysis. Frequency domain methods have very important difficulties related with the singularity encountered in the calculation of sound for a high speed body. Then time domain techniques are preferred.

The main purpose of this study is to refine the asymptotics of propeller noise of Parry and Crighton [3] for the subsonic case. For this reason, the asymptotics of Hanson's integral is carried out by using Laplace's method to second order. Using polynomial source distributions for loading and thickness noise, more refined formulas for far field noise are obtained. Results obtained using 4 bladed rotor propellers with SC1095 airfoil section show reduction of the far field noise by a few decibels.

## 2. EARLY THEORETICAL DEVELOPMENTS

In order to understand the more recent advances in helicopter noise prediction, it is helpful to go back to the late 1930s. The earliest methods used a point force model of the propeller for noise prediction. The first successful prediction theory was developed by Gutin [4] and the first theoretical result was obtained by using a stationary oscillating point force for calculating the first few harmonics of propeller noise due to blade loads. Later a thickness source was added. Ernsthausen in Germany [5] and Deming in the U.S. [6] recognized the importance of finite blade thickness. Garrick and Watkins [7] extended Gutin's result to propellers in forward flight in the early fifties. In the mid-fifties, Arnoldi [8] obtained an expression for thickness noise in the frequency domain. All of the early studies investigated only propeller noise.

In the 1960's, the noise of helicopters became an important issue. Initially both the piston engine and the rotor were the major generators of noise, but with the introduction of the turboshaft engine, the main and tail rotors became the dominant external noise sources because of the high speed of the rotor. It was realized that steady and unsteady blade surface pressure fluctuations were largely responsible for the discrete and broadband noise of the rotors, respectively [1]. However, the acoustic theories developed earlier for propellers were only applicable to hovering rotors because they did not include the unsteady blade loading. In practice, a hovering rotor has significant unsteady loading, hence, the propeller acoustics theories were inadequate even for hover. Some of the first noise prediction theories applied specifically to helicopter rotors were developed by Lawson [9] and Wright [10]. Lawson arrived at a simple, but powerful expression for a moving point source. At this time, the development of high speed digital computers helped the researcher to use more realistic models in their study. For instance, Lawson and Ollerhead [11] developed a computer code for rotor noise prediction both in time and frequency domains. Considerable experimental and theoretical studies have been carried out to understand the source mechanisms of helicopter rotors [12].

In 1952, Lighthill [13] introduced the acoustic analogy. In 1969 Ffowcs Williams and Hawkings published their now classic paper “Sound Generation by Turbulence and Surfaces in Arbitrary Motion” [14] which generalized Lighthill’s acoustic analogy approach [13] to include the effects of general types of surfaces and motions. Using the mathematical theory of distributions (also known as generalized functions), they were able to rearrange the Navier–Stokes equations into the form of an inhomogeneous wave equation with a quadrupole source distribution in the volume surrounding the body and monopole and dipole sources on the body surface. The Ffowcs Williams–Hawkings (FW–H) equation can be written in differential form as

$$\frac{\partial^2 p'}{\partial t^2} - c_o^2 \nabla^2 p' = \frac{\partial}{\partial t} [\rho_0 v_n \delta(f)] - \frac{\partial}{\partial x_i} [l_i \delta(f)] + \frac{\partial^2}{\partial x_i \partial x_j} [T_{ij} H(f)] \quad (2.1)$$

where  $p(x; t)$  is the acoustic pressure and the three source terms on the right-hand side are known as thickness, loading, and quadrupole source terms, respectively. The rotor blade is defined by the equation  $f = 0$ ,  $v_n$  is the local normal velocity of the surface,  $l_i$  are the components of the local force vector exerted by the surface on the fluid, and  $T_{ij}$  is Lighthill’s stress tensor. The FW-H equation is valid in the entire unbounded space. Hence, a formal solution may be obtained by using the free-space Green’s function  $\delta(g) / 4\pi r$ .

Ffowcs Williams and Hawkings paper encouraged theoretical work on helicopter rotor noise in the 1970’s. Hawkings and Lowson [15] and Farassat [16–17] applied the FW–H equation to the problem of rotor noise prediction. At this time acoustic code prediction development was limited by the lack of aerodynamic theories which were not sophisticated enough to satisfy the input requirements of the acoustic codes. The insight into noise generation aspect of high speed propeller was given by Jou [18] which was an extended version of the study of Lowson and Hawkings [15] in forward flight. Also Hanson [19] had successfully adapted his frequency domain method for aeroacoustic design of high speed propellers.

By the 1980's, theoretical development became more complicated to explain aerodynamically generated sound. In addition to that, several model scale and flight tests were carried out to understand and classify the physical sources of helicopter rotor noise. For instance, NASA/AHS Rotorcraft Noise Reduction Program (NR) [20] improved experimental data and theoretical understanding about sound generation. In parallel with the NR program, there were several high quality acoustic tests conducted in the German-Dutch wind tunnel (DNW) [21-22]. Farassat and Succi [23] predicted the transonic effects contained in the quadrupole term. Brentner [24] incorporated the Farassat and Succi formulation into NASA Langley's code, which is called WOPWOP. This code has been used for the prediction of helicopter rotor thickness and loading noise including detailed blade motion.

In 1990's, much of the research focused on the prediction of impulsive and broadband noise and the quadrupole term of the FW-H equation. Also, the Kirchhoff formulation for moving surfaces rapidly gained popularity [25], but later it was demonstrated that the FW-H equation is better than the Kirchhoff formula especially when used with a permeable surface surrounding all the sources [26]. In order to understand impulsive noise, Brentner and Farassat [27] developed a supersonic quadrupole formulation that did not have a Doppler singularity ( $1-M_r$ ) in the formulation. A recent publication by Howe gives a comprehensive account of rotor broadband noise prediction [28]. Ianniello [29,30] has also developed quadrupole noise prediction codes that integrate the FW-H equation on a supersonic rotating domain.

### 3. THEORETICAL BACKGROUND

#### 3.1 Lighthill's acoustic analogy

The Lighthill acoustic analogy [13] is obtained as follows. In the case of flow generated sound, the complete equations governing viscous fluid flow can be written as

$$\frac{\partial \rho}{\partial t} + \frac{\partial \rho u_i}{\partial x_i} = 0 \quad (3.1.1)$$

$$\frac{\partial \rho u_i}{\partial t} + \frac{\partial \rho u_i u_j}{\partial x_j} + \frac{\partial p}{\partial x_i} = \frac{\partial \tau_{ij}}{\partial x_j} \quad (3.1.2)$$

where  $\rho$  and  $p$  are the density and pressure, respectively and  $\tau_{ij}$  is the viscous stress tensor given by

$$\tau_{ij} = \mu \left\{ \frac{\partial u_i}{\partial x_j} + \frac{\partial u_j}{\partial x_i} - \frac{2}{3} \left( \frac{\partial u_k}{\partial x_k} \right) \delta_{ij} \right\} \quad (3.1.3)$$

By combining Eq. (3.1.1) and Eq. (3.1.2) using a procedure analogous to the development of the wave equation, an inhomogeneous wave equation is obtained as

$$\frac{\partial^2 \rho'}{\partial t^2} - c_0^2 \frac{\partial^2 \rho'}{\partial x_i \partial x_i} = \frac{\partial^2 T_{ij}}{\partial x_i \partial x_j} \quad (3.1.4)$$

where  $T_{ij} = \rho u_i u_j - \tau_{ij} + \delta_{ij} (p' - c_0^2 \rho')$  that is called Lighthill stress tensor. The perturbations are defined as the deviation from the uniform reference state  $(\rho_0, p_0)$ , namely

$$\rho' = \rho - \rho_0 \text{ and } p' = p - p_0 \quad (3.1.5)$$

Several points should be mentioned regarding the above derivation:

- a) No approximation has been made.
- b) At large distances away from the source region, Eq. (3.1.4) evolves into a linear wave equation. Accordingly, in the far field, the density and the pressure become the acoustic density and the acoustic pressure. In the near field, these quantities represent a combination of the hydrodynamic and acoustic/compressible fields.
- c) The original equation set contains four equations (continuity and the three scalar momentum equations) in five scalar unknowns, but Eq. (3.1.4) is a single equation with the same number of unknowns.

In conclusion, some assumptions or approximations must be made in order to investigate properly the sound generated.

In Lighthill's acoustic analogy, the right hand side of Eq. (3.1.4) is taken as the source of sound. One of the assumptions is that this term vanishes outside of the source region. Another approximation is related with Lighthill's stress tensor. Goldstein [31] provides a brief overview of  $T_{ij}$  in order to simplify this expression. One such approximation considers moderate to high flow Reynolds number. A second approximation is to assume that heat transfer is relatively unimportant in the flow. This implies an isentropic flow with  $p = c_0^2 \rho$ . As a result of these assumptions, Lighthill's stress tensor can be written as  $T_{ij} = \rho_0 u_i u_j$ . Additional approximation can be made by neglecting density fluctuations and using an incompressible approximation for  $u_i u_j$  so that  $T_{ij} = \rho_0 u_{0i} u_{0j}$ , where  $u_{0i}$  is the incompressible velocity component.

One of the big advantages of expressing the aeroacoustic problem in terms of an acoustic analogy is that the governing equation is linear and the right hand side can be simplified as described above. Lighthill's analogy was further generalized by Ffowcs Williams and Hawking [14] to account for moving surfaces, as discussed below.



### 3.2. The Ffowcs Williams–Hawkings equation

The FW–H equation [14] is an exact rearrangement of the continuity equation and the Navier–Stokes equations into the form of an inhomogeneous wave equation with two surface source terms and a volume source term. The FW–H equation is the most general form of the Lighthill acoustic analogy [13] because it extends the analogy to include general surfaces in arbitrary motion. The FW–H equation is the appropriate tool for predicting the noise generated by the complex motion of helicopter rotors. Today almost all deterministic rotor noise predictions are based on time-domain integral formulations of the FW–H equation.

The main ideas behind the derivation of the FW–H equation are as follows: Let a moving, impenetrable body (e.g., a propeller blade) be described by the equation  $f(\mathbf{x}; t) = 0$ , such that  $f > 0$  outside the body and  $\nabla f / |\nabla f| = \hat{n}$  (the unit outward normal to  $f = 0$ ) on the surface of the body. We assume that inside the body the fluid is at rest with the conditions of the quiescent medium (i.e., density  $\rho_0$  and sound speed  $c_0$ ). We have, therefore, introduced an artificial discontinuity in the field. Outside the body, the fluid has realistic flow properties which we assume are known. The right setting for studying this problem is the space of generalized functions [1]. As in the case of the Lighthill equation, we want to obtain a wave equation that is valid in the entire unbounded space. The conservation laws must be written with all derivatives as generalized derivatives [32]. We note that the conservation laws hold trivially inside  $f = 0$ . However, because of the artificial discontinuity in flow parameters introduced on  $f = 0$ , we must find the correction to the conservation laws. Note that in generalized function theory, the jump at the discontinuity of a function (and, hence, the memory of the jump) is retained in the generalized derivative.

The generalized mass conservation and momentum balance equations are

$$\frac{\partial \rho}{\partial t} + \frac{\partial}{\partial x_i}(\rho u_i) = \rho_0 v_n \delta(f) \quad (3.2.1)$$



$$\frac{\bar{\partial}}{\partial t}(\rho u_i) + \frac{\bar{\partial}}{\partial x_j}(\rho u_i u_j + P_{ij}) = l_i \delta(f) \quad (3.2.2)$$

where the bar over the derivatives on the left side denotes generalized differentiation,  $v_n = -\frac{\partial f}{\partial t}$  is the local normal velocity of the surface  $f = 0$  and  $l_i = P_{ij} n_j$  is the local force intensity (force/unit area) that acts on the blade surface. The Dirac delta function is denoted by  $\delta(f)$ . If we take  $\frac{\bar{\partial}}{\partial t}$  of Eq. (3.2.1) and  $\frac{\bar{\partial}}{\partial x_i}$  of (3.2.2) and subtract, we arrive at

$$\frac{\bar{\partial}^2 \rho'}{\partial t^2} - \frac{\bar{\partial}^2}{\partial x_i \partial x_j}(\rho u_i u_j + P_{ij}) = \frac{\bar{\partial}}{\partial t}[\rho_0 v_n \delta(f)] - \frac{\bar{\partial}}{\partial x_i}[l_i \delta(f)] \quad (3.2.3)$$

where the bars over the derivatives on the right side of the equation have been omitted.

Now, if we write  $p' = c_o^{-2} \rho'$ , subtract  $\frac{\partial^2 p'}{\partial x_i \partial x_j}$  from both sides, and rearrange the terms, FW-H equation can be written as follows,

$$\frac{1}{c_o^2} \frac{\bar{\partial}^2 p'}{\partial t^2} - \nabla^2 p' = \frac{\bar{\partial}}{\partial t}[\rho_0 v_n \delta(f)] - \frac{\bar{\partial}}{\partial x_i}[l_i \delta(f)] + \frac{\bar{\partial}^2}{\partial x_i \partial x_j}[T_{ij} H(f)] \quad (3.2.4)$$

where  $H(f)$  is the Heaviside function. The three terms on the right of equation (3.2.4) are known as the thickness, loading, and quadrupole sources, respectively [1].

Note that in FW-H equation, the thickness and loading source terms are surface distributions of sources (indicated by the presence of the Dirac Delta Function). These source terms have been used for several years in rotor noise prediction because they account for most of the acoustic signal when the flow field is not transonic and they do not require knowledge of the field around the blade (although the accurate determination of the blade-surface pressure is still challenging). The quadrupole source, on the other hand, is a volume distribution of sources (indicated by the Heaviside Function). However, the quadrupole source is often neglected in rotor noise prediction because of

the computational demands of computing the flow field with sufficient accuracy and integrating over a volume in the acoustic prediction [1].



#### 4. AERODYNAMIC COMPUTATION

The aerodynamic performance of a helicopter in hover flight is a first step to obtain generated noise level by rotor blade. Theoretically, a solution of the full Navier-Stokes equation with appropriate turbulence modeling and discretization scheme are sufficient for a good description of the flow field. A three dimensional body fitted computational grid is generated for a rectangular rotor blade with SC1095 airfoil section, as shown in Figure 4.1. The grids that are used here have 121 points in the wraparound direction, 43 points in the normal direction and 31 points in the spanwise direction (121x43x31). The grid was clustered near the leading and trailing edge and also near the tip region. Finite volume method is used to calculate the flow field by using ROE discretization scheme with the Spalart-Almaras turbulence model.

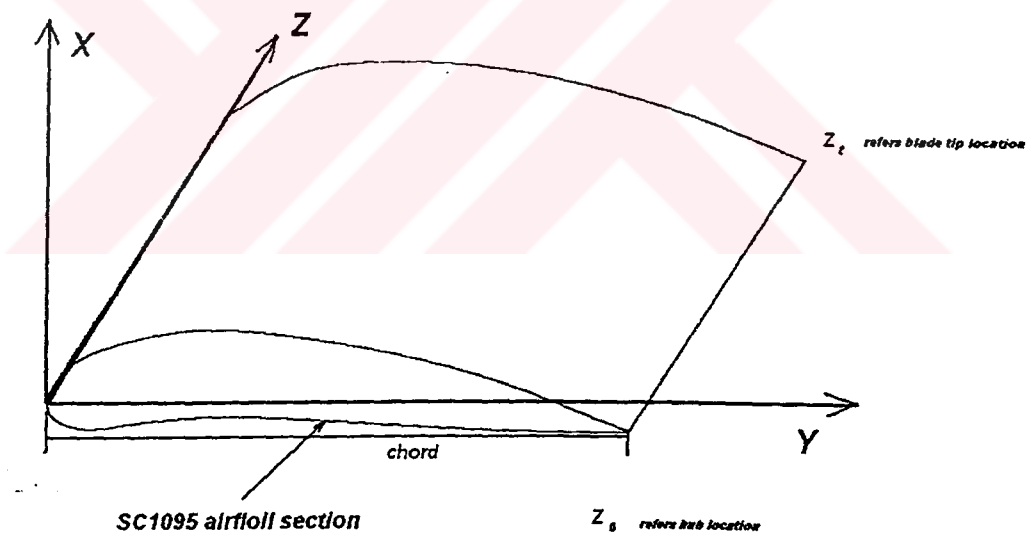


**Figure 4.1: Detailed airfoil description**

At the wall a no-slip boundary condition is used for the viscous calculation. The periodical boundary condition is used in the azimuthal direction. The angle of periodicity is given by  $2\pi/B$ , where  $B$  is the number of rotor blades. In this scheme, one dimensional blade element theory (see Figure 4.2) is used to approximate the inflow and outflow boundary conditions and  $2R$  away from the rotor blade in all directions.

The CFD computations are performed independently. As a result of this computation,  $C_p$ ,  $C_l$  and  $C_d$  values are taken as input to the aeroacoustic computation based on asymptotics.

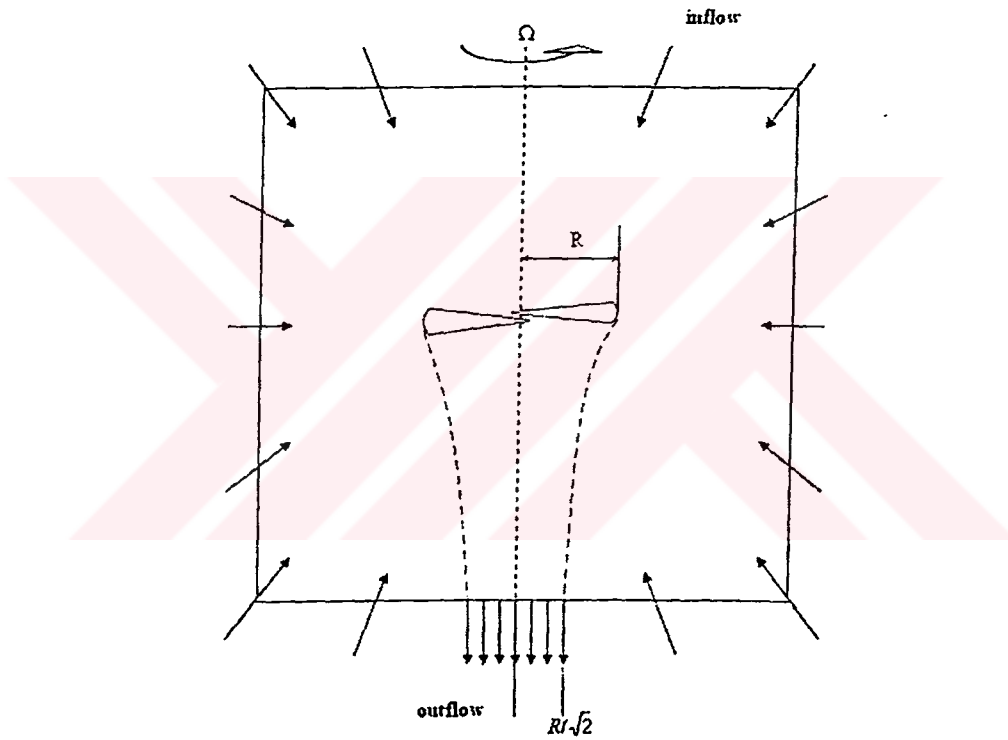


**Figure 4.2:** Boundary condition for aerodynamic calculation

In the 1-D momentum theory, the rotor is assumed as a point sink when viewed from far field. Using this theory, the far field normalized outflow velocity due to rotor system is related to the thrust by,

$$W_{out} = -2.M_t \sqrt{\frac{C_t}{2}} \quad (4.1)$$

where  $M_t$  is a tip Mach number and  $C_t$  is a thrust coefficient. This velocity is uniform and occurs below the rotor blade. A normalized inflow velocity at all boundaries equal to

$$W_{in} = -\frac{M_t}{4} \sqrt{\frac{C_t}{2}} \left(\frac{R}{r}\right)^2 \quad (4.2)$$

is used. Points are defined toward the hub of the rotor at all boundary locations [33]. According to these assumptions and boundary conditions, the computations are carried out and the results are discussed in Section 6.

## 5. ASYMPTOTIC THEORY OF PROPELLER NOISE

### 5.1 Hanson integral formula

The purpose of Hanson integral formulation [34] is to provide analytical expressions for understanding the sound generation mechanism and to determine the effects of parameters such as thickness, chord, sweep and airfoil section shape. Hanson started his formulation from the FW-H equation in the form of Goldstein's version [31]. The frequency domain formulation can be obtained by using a detailed mathematical transformation and expression. All steps can be found in Hanson's article [34].

The asymptotic theory is based on Hanson integral formulation in order to determine the sound field in the frequency domain. These formulas have a consistent structure for each source term, monopole and dipole (quadrupole term is not considered herein) and clearly separate the source strength from the acoustic interference effects due to radial and chordwise noncompactness and blade sweep.

The starting point for this investigation is the expression

$$p = \frac{-\rho c_0^2 DB}{8\pi r_0 (1 - M_x \cos \theta)} \sum_{m=-\infty}^{\infty} \exp \left[ \frac{imB\Omega}{(1 - M_x \cos \theta)} \left( t - \frac{r_0}{c_0} \right) + imB \left( \frac{\pi}{2} - \psi_0 \right) \right] \times \int_{z_0}^1 M_t^2 e^{-i\phi} J_{mB} \left[ \frac{mBM_t z \sin \theta}{(1 - M_x \cos \theta)} \right] \left( ik_y \frac{C_L}{2} \right) \Psi(k_x) dz \quad (5.1.1)$$

derived by Hanson [33] for the steady loading noise of a B-bladed SRP. Here  $\rho$  is the ambient density,  $p$  is the ambient pressure,  $c_0$  is the ambient speed of the sound,  $\Omega$  is the angular velocity of the rotor shaft,  $C_L$  is the lift coefficient of the blade,  $M_t$  and  $M_x$  are, respectively, the tip rotational Mach number and the forward flight Mach number,  $\theta$  is the radiation angle from propeller axis to observer point,  $D$  is the propeller diameter,  $r_0$  is the distance from the hub to the observer and  $\psi_0$  is the circumferential angle.

The rest of the symbols are defined as follows.

$$k_x = \frac{2mB(c/D)M_t}{(1 - M_x \cos \theta)M_r} \quad (5.1.2)$$

$$k_y = \frac{2mB(c/D)(M_r^2 \cos \theta - M_x)}{(1 - M_x \cos \theta)zM_r} \quad (5.1.3)$$

being nondimensional wave numbers  $k_x$  and  $k_y$ , and

$$\phi_s = \frac{2mB(s/D)M_t}{(1 - M_x \cos \theta)M_r} \quad (5.1.4)$$

is a phase contribution due to blade sweep.  $z$  is a normalized spanwise variable ( $z=1$  at the blade tip,  $z=z_0$  at the hub) and  $M_r = (M_x^2 + z^2 M_t^2)^{1/2}$  is the blade section relative Mach number. The propeller geometry is shown in Figure 5.1.

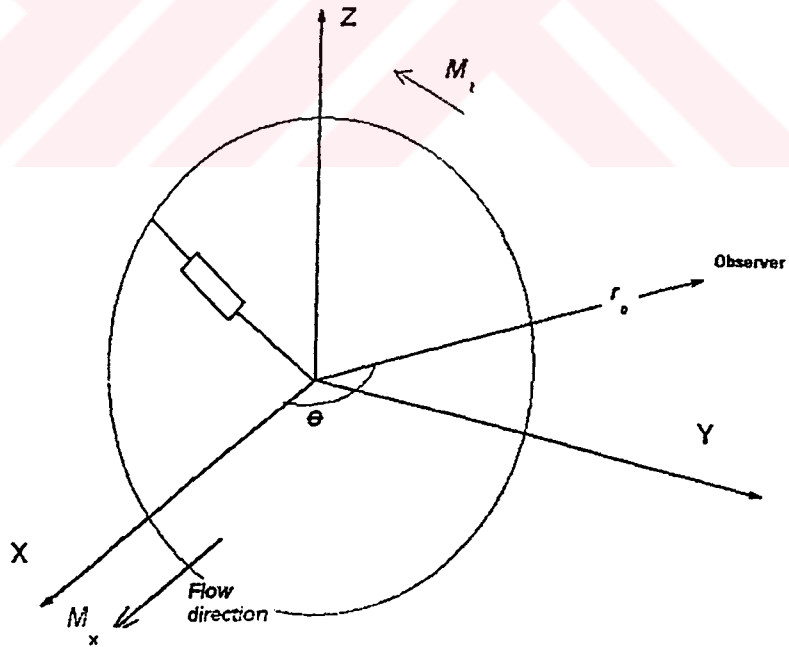


**Figure 5.1: Propeller geometry in the disk plane**

The chordwise non-compactness factors  $\Psi(k_x)$  for loading is given by

$$\Psi_L(k_x) = \int_{-1/2}^{1/2} F_L(X) e^{-ik_x X} dX \quad (5.1.5)$$

and  $\Psi(k_x)$  for thickness is given by

$$\Psi_V(k_x) = \int_{-1/2}^{1/2} h(X) e^{-ik_x X} dX \quad (5.1.6)$$

where  $h(X)$  and  $F_L(X)$  are, respectively, the normalized thickness and the lift distributions.

## 5.2. First order asymptotic approximation

Parry and Crighton [3] investigated propeller noise by the asymptotic theory for the prediction of steady loading dipole noise and thickness monopole noise for a single rotation propeller (SRP). The quadrupole noise term has been considered several times before in the context of propeller noise [35], the consensus is that quadrupole term may be ignored for thin or sweep blade operating away from the transonic regime.

Parry and Crighton carried out the analytical evaluation of the Hanson integrals by asymptotics. For the straight blade, a phase contribution due to blade sweep is set equal to zero,  $\Phi_s=0$  and  $\Psi_L = \Psi_V = I$  because chordwise noncompactness factors are not important for low and moderate subsonic speeds.

With these assumptions, equation (5.1.1) can be written in the harmonic components of the sound field as

$$p = \frac{-\rho c_0^2 DB}{8\pi r_0 (1 - M_x \cos \theta)} \sum_{m=-\infty}^{\infty} \exp \left[ \frac{imB\Omega}{(1 - M_x \cos \theta)} \left( t - \frac{r_0}{c_0} \right) + imB \left( \frac{\pi}{2} - \psi_0 \right) \right] P_m \quad (5.2.1)$$

where  $P_m$  is  $m$ th harmonic component of the sound field and is given by



$$P_m = \int_{z_0}^1 S_m(z) J_{mB} \left[ \frac{mBM_t z \sin \theta}{(1 - M_x \cos \theta)} \right] dz \quad (5.2.2)$$

where  $J_n$  denotes the Bessel function of the first kind of order  $n$ , representing the radiation efficiency of sources rotating in the nominal disk plane [3] and where  $S_m(z)$  represents the variation in source strength in spanwise direction.  $S_m(z)$  is different for loading and thickness cases and depends on the harmonic number  $m$ , blade number  $B$  and the propeller operating parameters. The source strength of loading is given by

$$S_m(z) = M_r^2 \left( ik_y \frac{C_L}{2} \right) \quad (5.2.3)$$

and the source strength of thickness is given by

$$S_m(z) = M_r^2 \left( k_x^2 \frac{b}{c} \right) \quad (5.2.4)$$

for the subsonic case. If the order of the Bessel function  $mB$  is assumed to be large, the Debye approximation [36] holds:

$$J_{mB}(mB \sec h\beta) \approx \frac{\exp[mB(\tanh \beta - \beta)]}{(2\pi mB \tanh \beta)^{1/2}} \quad (5.2.5)$$

where

$$\sec h\beta = \frac{zM_t \sin \theta}{(1 - M_x \cos \theta)} \quad (5.2.6)$$

Using the Debye approximation, Eq. (5.2.2) can be evaluated using Laplace's method. Parry-Crighton [3], use a power law source distribution in the form,

$$S(z) \approx \bar{S}(1-z)^\nu \text{ as } z \rightarrow 1 \quad (5.2.7)$$

to arrive at

$$P_m \approx \frac{\bar{S} \exp[mB(\tanh \beta_t - \beta_t)]}{(2\pi mB \tanh \beta_t)^{1/2}} \int_{-\infty}^1 (1-z)^\nu \exp[-mB(1-z) \tanh \beta_t] dz \quad (5.2.8)$$

where

$$\beta_t = \sec h^{-1} \left[ \frac{M_t \sin \theta}{(1 - M_x \cos \theta)} \right] \quad (5.2.9)$$

and the subscript t refers to the blade tip. Eq. (5.2.8) can then be evaluated to give

$$P_m \approx \frac{\bar{S} \exp[mB(\tanh \beta_t - \beta_t)]}{(2\pi mB \tanh \beta_t)^{1/2}} \frac{\Gamma(\nu+1)}{(mB \tanh \beta_t)^{\nu+1}}. \quad (5.2.10)$$

If the source strength is taken to be finite at the propeller tip, then  $\bar{S} = S(1)$ ,  $\nu = 0$ . Parry and Crighton obtained  $\bar{S}$  and  $\nu$  by matching Eq. (5.2.7) with the variation of the radial loading distribution.

In the present study, we use a polynomial fit to the aerodynamic loading in the form

$$S(z) = \sum_{\nu=0}^N \bar{S}_\nu (1-z)^\nu \quad (5.2.11)$$

where  $\bar{S}_\nu$ ,  $\nu=0,1,\dots,N$  are to be obtained by fitting to CFD computations. In this case, the first order approximation of Parry-Crighton for the  $m$ th harmonic far field pressure  $P_m$  takes the form

$$P_m \approx \frac{\exp[mB(\tanh \beta_t - \beta_t)]}{(2\pi mB \tanh \beta_t)^{1/2}} \sum_{\nu=0}^N \bar{S}_\nu \frac{\Gamma(\nu+1)}{(mB \tanh \beta_t)^{\nu+1}} \quad (5.2.12)$$

The asymptotic formula of the  $m$ th harmonic for loading of the far field acoustic depends on the tip rotational Mach number  $M_t$ , the radiation angle  $\theta$  and the aerodynamic lift distribution (through  $\bar{S}_\nu$ ) for loading.

### 5.3. Second order asymptotic approximation

The starting point for the second order approximation is Eq. (5.2.2) in the Debye approximation, namely

$$P_m = \int_{z_0}^1 S(z) \frac{\exp[mB(\tanh \beta - \beta)]}{(2\pi mB \tanh \beta)^{1/2}} dz. \quad (5.3.1)$$

If we define

$$\lambda = mB \text{ and } F[\beta(z)] = \tanh \beta - \beta, \quad (5.3.2-3)$$

then Eq.(5.3.1) becomes

$$P_m = \int_{z_0}^1 S(z) \frac{e^{\lambda F[\beta(z)]}}{(2\pi mB \tanh \beta)^{1/2}} dz \quad (5.3.4)$$

where

$$\sec h\beta = \frac{zM_t \sin \theta}{(1 - M_x \cos \theta)} = z\kappa \quad \text{with} \quad \kappa = \frac{M_t \sin \theta}{(1 - M_x \cos \theta)} \quad (5.3.5)$$

In the limit  $\lambda \rightarrow \infty$ , by Laplace's method, the major contribution to the integral arises from the immediate vicinity of the tip ( $z=1$ ).  $F[\beta(z)]$  can now be expanded in a Taylor series about  $z=1$  since the integrand of Eq.(5.3.1) increases rapidly towards the tip [3].

A Taylor series expansion of  $F[\beta(z)]$  about the tip ( $z=1$ ) yields

$$F[\beta(z)] = F[\beta(1)] + \left. \frac{dF[\beta(z)]}{dz} \right|_{z=1} (z-1) + \left. \frac{d^2 F[\beta(z)]}{dz^2} \right|_{z=1} \frac{(z-1)^2}{2!} + O[(z-1)^3] \quad (5.3.6)$$

The derivatives of  $F$  can be obtained using the chain rule so that

$$\frac{dF}{dz} = \frac{dF}{d\beta} \frac{d\beta}{dz} = \kappa \sinh \beta \quad (5.3.7a)$$

$$\frac{d^2 F}{dz^2} = \frac{d^2 F}{d\beta^2} \left( \frac{d\beta}{dz} \right)^2 + \frac{d^2 \beta}{dz^2} \frac{dF}{d\beta} = -\kappa^2 \frac{\cosh^3 \beta}{\sinh \beta} \quad (5.3.7b)$$

Substituting Eq. (5.3.7a) and Eq. (5.3.7b) into Eq.(5.3.6), we get

$$F[\beta(z)] = \tanh \beta_i - \beta_i + \kappa \sinh \beta_i (z-1) - \kappa^2 \frac{\cosh^3 \beta_i}{\sinh \beta_i} \frac{(z-1)^2}{2!} + \dots + O[(z-1)^3] \quad (5.3.8)$$

Eq. (5.3.4) can be rewritten using the polynomial source description, Eq. (5.2.11), as

$$P_m = \frac{\exp[\lambda \tanh \beta_i - \beta_i]}{(2\pi \lambda \tanh \beta_i)^{1/2}} \sum_{v=0}^N \bar{S}_v \int_{-\infty}^1 (1-z)^v \exp[-\lambda \{ \kappa \sinh \beta_i (1-z) - \kappa^2 \frac{\cosh^3 \beta_i}{\sinh \beta_i} \frac{(1-z)^2}{2} \}] dz \quad (5.3.9)$$

If we let  $1-z=u$  in the integral of Eq. (5.3.9) and define  $I_v$  by

$$I_v = \int_0^1 u^v \exp[-\lambda \kappa \sinh \beta_i u - \lambda \kappa^2 \frac{\cosh^3 \beta_i}{\sinh \beta_i} \frac{u^2}{2}] du \quad (5.3.10)$$

the transformation  $\sqrt{\lambda \kappa^2 \frac{\cosh^3 \beta_i}{\sinh \beta_i}} u = s$  yields

$$I_v = \frac{1}{\left[ \lambda \kappa^2 \frac{\cosh^3 \beta_i}{\sinh \beta_i} \right]^{\frac{v+1}{2}}} \int_0^{\infty} s^v \exp[-\alpha s - \frac{1}{2} s^2] ds \quad (5.3.11)$$

$$\text{where } \alpha = \frac{\lambda \tanh \beta_i}{\sqrt{2 \lambda \kappa^2 \frac{\cosh^3 \beta_i}{\sinh \beta_i}}} \quad (5.3.12)$$

From Abromowitz and Stegun [36], we have

$$U(a, z) = D_{-a-\frac{1}{2}}(z) = \frac{1}{\Gamma(\frac{1}{2}+a)} \exp\left[\frac{z^2}{4}\right] \int_0^{\infty} \exp\left[-zt - \frac{1}{2}t^2\right] t^{a-\frac{1}{2}} dt \quad (5.3.13)$$

when  $a + \frac{1}{2}$  is a positive integer.

Comparing Eq. (5.3.11) and Eq. (5.3.13), we can identify  $\nu = a - \frac{1}{2}$  and  $z = \alpha$  so that

$$\int_0^{\infty} s^{\nu} \exp\left[-\alpha s - \frac{1}{2}s^2\right] ds = \exp\left[\frac{\alpha^2}{4}\right] D_{-\nu-1}(\alpha) \Gamma(1+\nu) \quad (5.3.14)$$

In Eq. (5.3.11), the term in front of the integral sign can be rearranged as

$$\frac{1}{\left[\lambda \kappa^2 \frac{\cosh^3 \beta_i}{\sinh \beta_i}\right]^{\frac{\nu+1}{2}}} = \frac{\alpha^{\nu+1}}{(\lambda \tanh \beta_i)^{\nu+1}}$$

by using the definition of  $\alpha$ , Eq. (5.3.12), so that

$$P_m = \frac{\exp[\lambda(\tanh \beta_i - \beta_i)]}{(2\pi\lambda \tanh \beta_i)^{1/2}} \sum_{\nu=0}^N \bar{S}_{\nu} \frac{\Gamma(1+\nu)}{(\lambda \tanh \beta_i)^{\nu+1}} \alpha^{\nu+1} D_{-\nu-1}(\alpha) \exp\left[\frac{\alpha^2}{4}\right] \quad (5.3.15)$$

This is the second order asymptotic formula for the  $m$ th harmonic of the far field acoustic pressure of a  $B$ -bladed propeller in the asymptotic limit  $\lambda = mB \rightarrow \infty$ .

## 6. RESULTS AND DISCUSSION

A commercial computational fluid dynamic (CFD) code is used to compute the aerodynamic loading. The code was first validated in comparison with CFD results of Wake and Baeder [37]. Analysis is applied to 3-to-1 tapered tip blade in hover and the results are compared with experimental data [38]. Comparisons are shown for different radial stations in Figures 6.1-6.3.

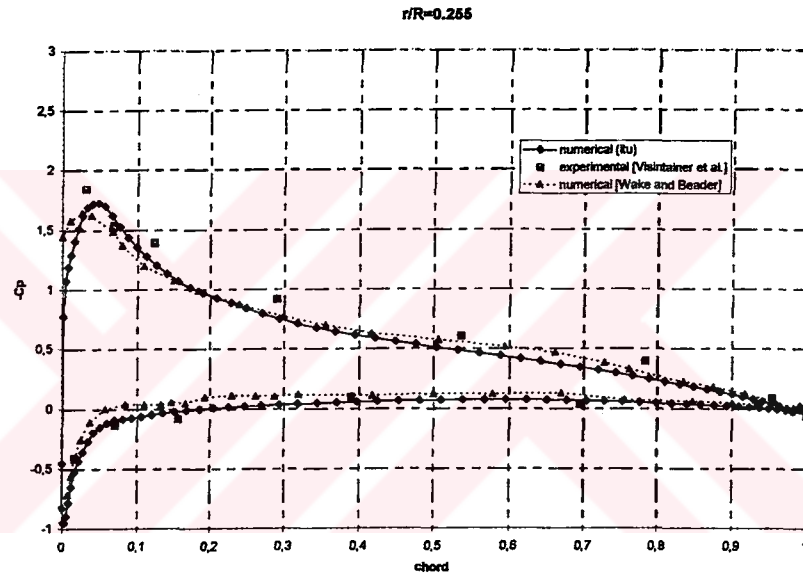


**Figure 6.1:**  $C_p$  distribution of 3-to-1 tapered tip blade along chordwise direction at  $r/R_0=0.225$ .

For the validation case, the computation is performed using  $121 \times 43 \times 31$  mesh points with finer resolution near the tip and a minimum normal spacing of  $0.00004c$ . The minimum spacing in the radial direction is  $0.002R$  at the tip. The Reynolds number,  $Re$ , based on the chord length, is  $2.75 \times 10^6$ , and the tip Mach number  $M_t$  is  $0.628$ .

The results are compared at different stations along the spanwise direction at  $r/R=0.255$ ,  $0.775$  and  $0.945$  and are shown in Figures 6.1-6.3. The numerical results obtained by the standard commercial code at different radial stations for the chordwise pressure

coefficient  $C_p$  on the blade show good agreement with those of experimental and of Wake and Baeder, suggesting that it can be employed to compute aerodynamic loading.

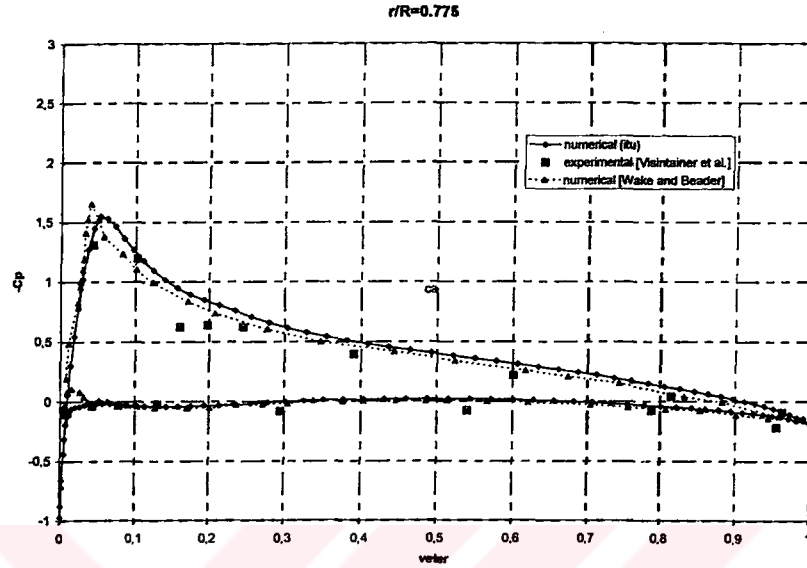


Figure 6.2:  $C_p$  distribution of 3-to-1 tapered tip blade along chordwise direction at  $r/R_0=0.775$

The hovering performance of a helicopter rotor is calculated using a four-bladed straight planform with tip Mach numbers ranging between 0.5 and 0.7 in order to determine aerodynamic loading.

The aerodynamic results are then fitted by using the least squares method for a polynomial fit to identify the source strength. In Figure 6.4, the pressure coefficient distribution is given for  $M_t=0.5$  along spanwise direction at five different stations for a straight planform blade to predict noise level and to make comparison between the Parry-Crighton formula and the present refined equation, Eq. (2.3.15).

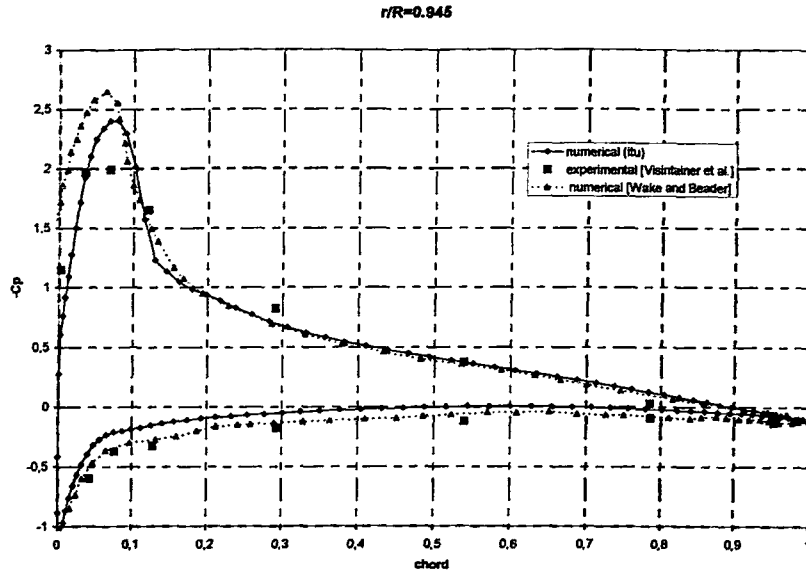


Figure 6.3:  $C_p$  distribution of 3-to-1 tapered tip blade along chordwise direction at  $r/R_0=0.945$

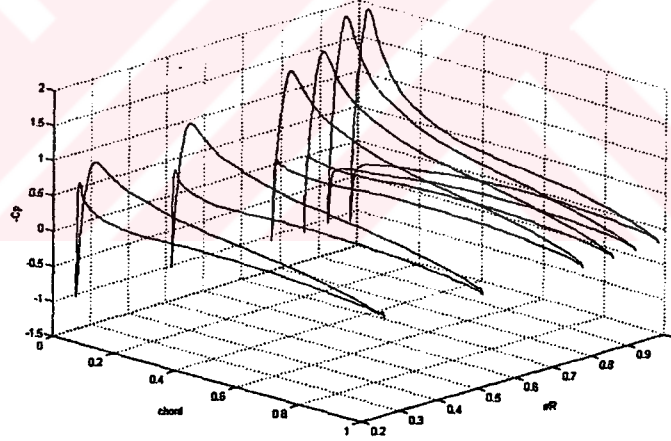
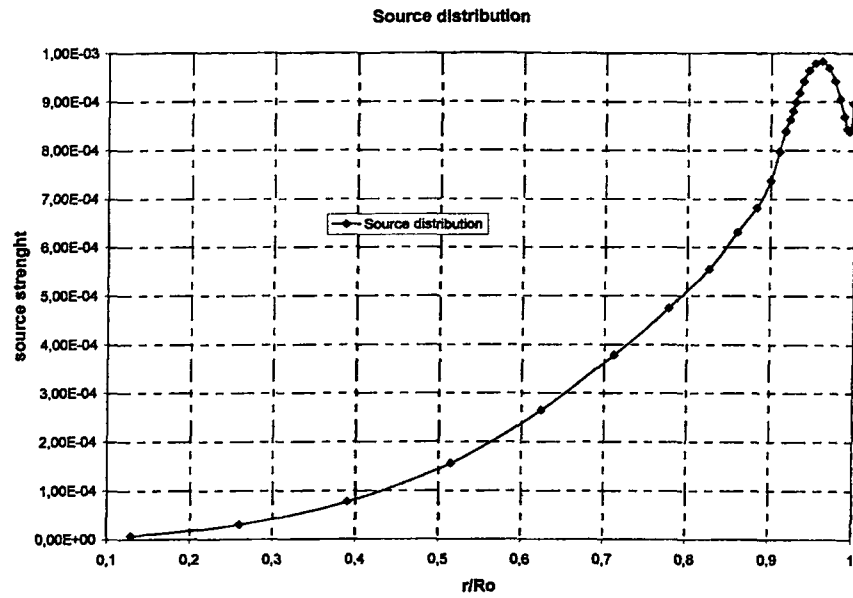


Figure 6.4:  $C_p$  distribution of rectangular planform blade along radial direction in hover for the computation of noise prediction

According to the result of  $C_p$  for aerodynamic loading, the source strength  $S_m(z)$  can be calculated by using Eq. (5.2.3) for all harmonics. The results are shown in Figure 6.5.





**Figure 6.5:** Source strength  $S_m(z)$  distribution for aerodynamic loading along spanwise direction

Polynomial fitting with degrees of  $v=2$  and  $v=3$  to the CFD results for aerodynamic loading are shown in Figure 6.6. A better fit is obtained for  $v=2$ .

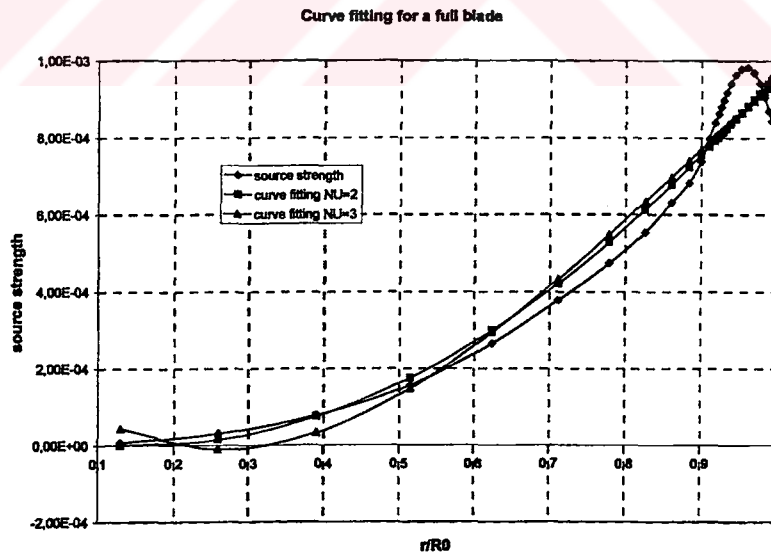


**Figure 6.6:** Polynomial fitting of the source strength  $S_m(z)$  for aerodynamic loading by the method of least squares (NU is the degree of the polynomial)

Figure 6.7 compares the results of the Parry-Crighton equation and those of the second order refined equation of present study for steady loading noise prediction along the blade for a polynomial fit of degree  $\nu=2$ .

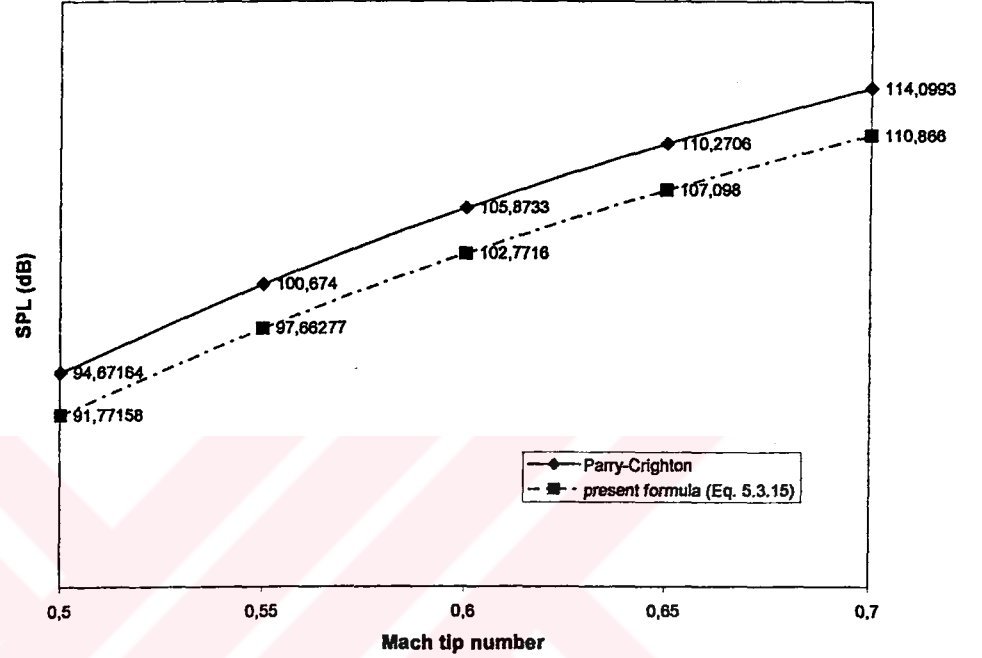


**Figure 6.7:** Comparison of asymptotic predictions for aerodynamic loading between Parry-Crighton [3] and the present work for the SPL (dB) for an observer located at  $r_o=141.421$  m with a radiation angle  $\theta=89.88^\circ$ .

In the far field, the observer is located near the rotation plane of the rotor with coordinates given by (100 m, 100 m, 0.3 m) in x,y,z directions, respectively. The distance between the observer and the hub is equal to  $r_o=141.421$  m and the radiation angle is equal to  $\theta=89.88^\circ$ .

A convergence test for the Parry-Crighton formula and for the present work was conducted and the results for  $M_t=0.5$  are shown in Figure 6.8. It is clear that there is a good shape agreement between Parry-Crighton and the present second order refined expression. The present results show nearly 3 dB reduction in SPL in comparison with those of the Parry-Crighton formula.

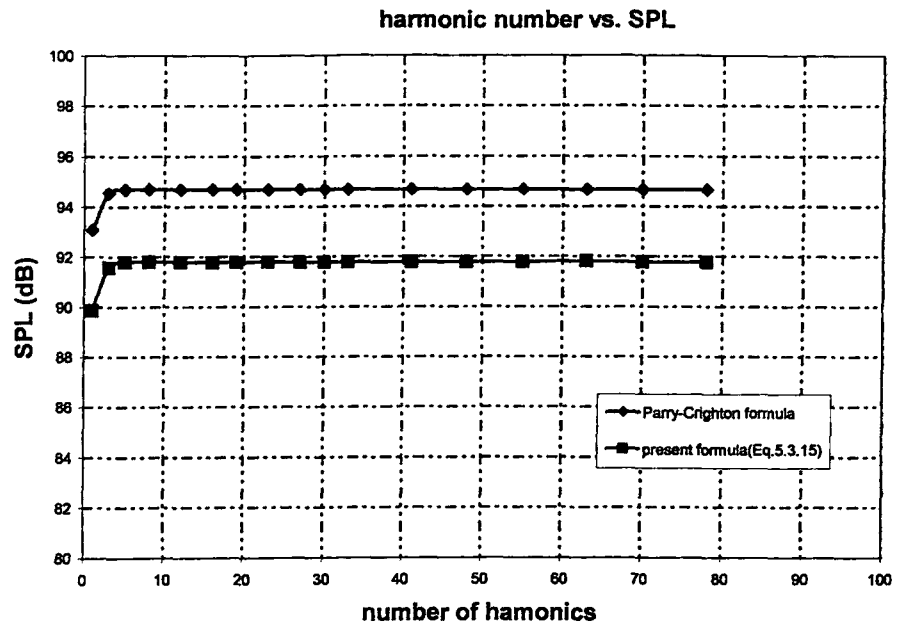


**Figure 6.8:** Comparison of harmonic convergence at tip Mach number  $M_t=0.5$  between Parry-Crighton [3] and the present work for the SPL (dB) for an observer located at  $r_o=141.421$  m with a radiation angle  $\theta=89.88^\circ$  for higher harmonic numbers

## 7. CONCLUSION

This study has used the asymptotic theory for the noise prediction of a subsonic  $B$ -bladed helicopter rotor blade. The Hanson integral formula is used to investigate the rotor blade noise. Using the Debye approximation for Bessel functions with large order, the resulting integral is evaluated by Laplace's method. In particular, a polynomial source strength in the form,

$$S = \sum_{\nu=0}^N \bar{S}_{\nu} (1-z)^{\nu} \quad (7.1)$$

is used to fit the aerodynamic loading and second order corrections to the asymptotic theory of single rotational propeller noise are considered refining the harmonic components  $P_m$  of the radiation sound field as

$$P_m = \frac{\exp[\lambda(\tanh \beta_t - \beta_t)]}{(2\pi\lambda \tanh \beta_t)^{1/2}} \sum_{\nu=0}^N \bar{S}_{\nu} \frac{\Gamma(1+\nu)}{(\lambda \tanh \beta_t)^{\nu+1}} \alpha^{\nu+1} D_{-\nu-1}(\alpha) \exp\left[\frac{\alpha^2}{4}\right] \quad (7.2)$$

using thickness and loading source terms only.

A 3D compressible CFD code is used to compute the aerodynamic loading on the blade for a four bladed helicopter rotor in hover. For this case, the tip Mach number is chosen in the range between 0.5 and 0.7. When aerodynamic loading data is fitted to the source strength according to Eq. (7.1), it is shown that the SPL noise prediction is reduced by the present second order formula nearly 3dB.

In the subsonic propeller noise prediction problem, the near field acoustic pressure is also important and that subject will be investigated in future work. In noise generation, the problem is defined according to the source characteristics i.e linear or nonlinear. The linear case is considered here using steady loading and thickness noise terms. In the

nonlinear case, the quadrupole source term becomes important because it represents nonlinear effects arising from the flow field such as shock structure and turbulence.



## REFERENCES

- [1] Brentner, K.S. and Farassat, F., 1994. Helicopter noise prediction: the current status and future direction. *Journal of Sound and Vibration*, 170, 79–96.
- [2] Carley, M., 1996. Time domain calculation of noise generated by a propeller in a flow, *PhD Thesis*, Trinity College, Dublin, Ireland.
- [3] Parry, A. B. and Crighton, D. G., 1989. Asymptotic theory of propeller noise part I: Subsonic single rotation propeller, *AIAA Journal*, 27, 1184–1190.
- [4] Gutin, L., 1936. On the sound of a rotating airscrew, *Z Tech Fiz*, 6, 889–909 [translated as NACA TM 1192, 1948].
- [5] Ernsthausen, W., 1936. The source of propeller noise, *Luftfahrtforschung*, 8, 433–440 [translated as NACA Report, TM 825, 1937].
- [6] Deming, A.F., 1938. Noise from propellers with symmetrical sections at zero blade angle, II, *NACA Report*, TM 679.
- [7] Garrick, I.E. and Watkins, C.E., 1954. A theoretical study of the effect of forward speed on the free-space sound-pressure field around propellers, *NACA Report*, 1198.
- [8] Arnoldi, R.A., 1956. Propeller noise caused by blade thickness, *Unite Aircraft Corporation Research Department Report*, R-896.
- [9] Lowson, M.V., 1965. The sound field of singularities in motion, *Proceedings of the Royal Society of London. Series A: Mathematical and Physical Sciences*, 286, 559–572.
- [10] Wright, S.E., 1969. Sound radiation from a lifting rotor generated by asymmetric disc loading, *Journal of Sound and Vibration*, 9, 223–240.
- [11] Lowson, M.V. and Ollerhead, J.B., 1969. A theoretical study of helicopter rotor noise, *Journal of Sound and Vibration*, 9, 197–222.
- [12] Lowson, M.V., 1973. Helicopter noise: analysis-prediction and methods of reduction, *AGARD Report*, LS-63.
- [13] Lighthill, M.J., 1952. On Sound Generated Aerodynamically I: General Theory, *Proceedings of the Royal Society. Series A*, 221, pp. 564–587.

- [14] Ffowes Williams, J.E. and Hawkings, D.L., 1969. Sound Generated by Turbulence and Surfaces in Arbitrary Motion, *Philosophical Transactions of the Royal Society. Series A*, 264, No.1151, pp. 321–342.
- [15] Hawkings, D.L. and Lowson, M.V., 1974. Theory of open supersonic rotor noise, *Journal of Sound and Vibration*, 36, 1–20.
- [16] Farassat, F., 1975. Theory of noise generation from moving bodies with an application to helicopter rotors, *NASA Report*, TR R-451.
- [17] Farassat, F., Pegg, R.J. and Hilton, D.A., 1975. Thickness noise of helicopter rotors at high tip speeds, *AIAA Paper* 75-453.
- [18] Jou, W.H., 1979. Supersonic propeller noise in a uniform flow, *AIAA Paper* 79-0348.
- [19] Hanson, D.B., 1980. Influence of propeller design parameters on far field harmonic noise in forward flight, *AIAA Journal*, 18, 1313-1319
- [20] Levertton, J.W., 1989. Twenty-five years of rotorcraft aeroacoustics: Historical prospective and important issues, *Journal of Sound and Vibration*, 133, 261-287.
- [21] Martin, R.M. and Splettstoesser, W.R., 1988. Blade–vortex interaction acoustic results from a forty percent model rotor in the DNW. *Journal of the American Helicopter Society*, 33, 37–46.
- [22] Brooks, T.F., Marcolini, M.A. and Pope, D.S., 1989. Main rotor broadband noise study in the DNW, *Journal of the American Helicopter Society*, 34, 3–12.
- [23] Farassat, F. and Succi, G.P., 1983. The prediction of helicopter discrete frequency noise, *Vertica*, 7, 309–20.
- [24] Brentner, K.S., 1986. Prediction of helicopter discrete frequency rotor noise; a computer program incorporating realistic blade motions and advanced acoustic formulation, *NASA TM* 87721.
- [25] Lyrantzis, A.S., 1994. Review - The use of Kirchoff's method in computational aeroacoustics, *Journal of Fluids Engineering*, 116, 665-676.
- [26] Brentner, K.S. and Farassat, F., 1998. An analytical comparison of the acoustic analogy and Kirchhoff formulation for moving surfaces, *AIAA J.*, 36, 1379–1386.

- [27] **Farassat, F. and Brentner, K.S.**, 1998. Supersonic quadrupole noise theory for high-speed helicopter rotors, *Journal of Sound and Vibration*, **218**, 481–500.
- [28] **Howe, M.S.**, 1999. Trailing edge noise at low Mach numbers, *Journal of Sound and Vibration*, **225**, 211–238.
- [29] **Ianniello, S.**, 1999. Quadrupole noise predictions through the FW–H equation, *AIAA*, **37**, 1048–1054.
- [30] **Ianniello, S.**, 2001. Aerocooustic analysis of high tip speed rotating blades, *Aerospace Science Technology*, **5**, 179–192.
- [31] **Goldstein, M.E.**, 1976. *Aeroacoustics*, McGraw-Hill International Book Company, New York.
- [32] **Kanwal, R.P.**, 1998. *Generalized functions—theory and technique*, 2nd ed. Boston: Birkhauser.
- [33] **Leishman, J. G.**, 2000. *Principles of Helicopter Aerodynamics*, Cambridge University Press.
- [34] **Hanson, D. B.**, 1980. Hellicoidal surface theory for harmonic noise of propellers in the far field, *AIAA*, **18**, 1213–1220.
- [35] **Hanson, D.B. and Fink, M.R.**, 1979. The importance of quadrupole sources in prediction of transonic tip speed propeller noise, *Journal of Sound and Vibration*, **62**, 19–38.
- [36] **Abramowitz, M. And Stegun, I. A.**, 1965. *Handbook of mathematical function*, Dover Publications, Inc, New York.
- [37] **Wake, B. E. and Baeder, J. D.**, 1996. Evaluation of a Navier-Stokes analysis method for hover performance prediction, *Journal of the American Helicopter Society*, **41**, 7–17.
- [38] **Visintainer, J.A., Marcolini, M.A., Burley, C.L., and Liu, S.R.**, 1993. Acoustic Predictions Using Measured Pressures from a Model Rotor in the DNW, *Journal of the American Helicopter Society*, **38**, 35–44.



## **CURRICULUM VITAE**

Baha ZAFER was born in Istanbul in 1978. He graduated from İstanbul Technical University with major in Astronautical Engineering in 2002. He has been a research assistant in the Program of Advanced Technologies in Engineering.

